

## **SUB-MODELLING AND BOUNDARY CONDITIONS WITH *P*-TYPE HYBRID-EQUILIBRIUM PLATE-MEMBRANE ELEMENTS**

A.C.A. Ramsay\*<sup>1</sup> and E.A.W. Maunder<sup>2</sup>

\* Corresponding author

1 A.C.A. Ramsay - *Tel:* +44-1522-545830 *E-mail address:* [angus\\_ramsay@yahoo.co.uk](mailto:angus_ramsay@yahoo.co.uk)

PCA Engineers Limited, Homer House, Sibthorp Street, Lincoln, LN5 7SB, England

2 E.A.W. Maunder - *Tel:* +44-1392-263634 *E-mail address:* [e.a.w.maunder@exeter.ac.uk](mailto:e.a.w.maunder@exeter.ac.uk)

University of Exeter, Department of Engineering, School of Engineering, Computer Science and Mathematics, North Park Road, Exeter, EX4 4QF, England

---

### **Abstract**

The main topics of this paper, sub-modelling and associated boundary conditions, are presented in two parts. The first part details a general method for evaluating consistent displacement or traction modes for hybrid equilibrium plate models to represent arbitrarily specified boundary conditions. The inheritance of boundary conditions in a process of uniform  $h$ -type refinement is considered as a particular case. The second part investigates the methodology and performance of a sub-modelling technique involving equilibrium elements which has the aim of recovering a local quantity of interest with greater accuracy than that directly obtained from the original global or parent equilibrium model. A crucial step in this technique is the transfer of appropriate boundary tractions from the parent model to the sub-model (child). The sub-modelling technique is presented initially based on the extraction of a single element for  $h$ - and/or  $p$ -type refinement into sub-models. A more general form of sub-modelling is then presented in which the boundary of the sub-model does not coincide with that of an element, or patch of elements, in the parent model. This requires the evaluation of modes of traction around an arbitrary region, and a scheme to achieve this is presented and demonstrated using, as an example, a geometric perturbation of a single element extraction. The performances of sub-models are compared using both complete sets of traction modes and reduced, or basic, sets.

*Keywords:* Static and kinematic Boundary conditions; Sub-modelling technique; Hybrid-stress elements; Equilibrium elements;  $P$ -type; Plate-membrane problems

---

## 1. INTRODUCTION

Hybrid-stress or *equilibrium* elements are a particular type of finite element (FE) which can provide *statically admissible* solutions to problems in structural mechanics. The formulation of such elements is more complicated than that of conventional displacement elements but the value of obtaining solutions for which the stress field is in equilibrium in a pointwise sense throughout the model is considered to justify this additional complexity. In particular, many structural design criteria involve placing upper limits on the value of static variables, e.g. the so-called membrane and bending stresses used in, *inter alia*, pressure vessel design codes, e.g. ASME [1]. With equilibrium elements the amplitudes of these variables form part of the basic solution and do not require additional post-processing as in the displacement method. Unlike displacement models, for equilibrium models these static variables are also in equilibrium with the applied loads. In conjunction with the lower-bound theorem of plasticity, equilibrium elements also provide a natural route to obtaining safe solutions to structural problems. Equilibrium elements have also found use in error estimation for conventional displacement elements [2] and from the viewpoint of the practicing engineer offer a more intuitive or natural approach to finite element analysis (FEA) [3].

The equilibrium element considered in this paper is a variable degree or  $p$ -type plate-membrane element the basic theory of which was presented in [4]. Other equilibrium elements such as axisymmetric, [5], plate-bending, [6], and solid continuum, [7], are available, and much of the work presented in this paper is directly applicable to those other element types. The equilibrium element differs from many conventional elements in that the degrees of freedom are referred to element edges rather than to nodes. The consistent method of applying boundary conditions then involves the specification of distributions of edge displacement and/or traction. Section 2 presents a method of calculating these distributions for

arbitrarily defined displacement and stress fields and provides examples of force and displacement driven problems. The inclusion of such a facility, similar to the Continuum-Region-Element method [8,9], in a FE program enables the user both to develop an understanding of the approximation inherent in the particular form of element being used and, also, offers a program that can provide its own validation problems. In closing Section 2 it is noted that most routine application of FEA involves specifying nothing more than the so-called *basic traction distributions* (or modes) which correspond directly to resultant forces and moments.

Section 3 investigates the methodology and performance of the *sub-modelling technique* as applied to equilibrium elements. In structural FEA sub-modelling is often used [10] to obtain accurate stresses from a refined or *sub-model* of the region of interest with boundary conditions applied from the results of a coarser global or *full-model*. For displacement-based models, where the basic solution is a piecewise continuous displacement field, the most direct form of boundary conditions for the sub-model are displacements or kinematic boundary conditions (KBCs) obtained by interpolation of the full-model displacement field along the boundaries of the sub-model. In contrast, for equilibrium elements, where the basic solution is a piecewise statically admissible stress field, the natural form of boundary conditions for the sub-model are boundary tractions or static boundary conditions (SBCs) obtained by evaluating the tractions corresponding to the full-model stress field along the boundaries of the sub-model. The sub-modelling technique for the equilibrium element is first established using a sub-model consisting of a single element extracted from the full-model. Adopting this so-called *element-extraction* approach, two forms of sub-model refinement, *viz.* *p-type* and *h-type*, are considered [11]. With *h-type* refinement the refined sub-model needs to inherit the boundary conditions of the original sub-model discussed in the

first part of the paper. The performance of the sub-model is evaluated using both the complete set of traction modes and a reduced or basic set. In contrast to the element extraction method, the boundaries of a general sub-model will cut across the interior of elements in the full-model and although satisfying interelement equilibrium, the stress fields are not generally continuous across such interfaces. The tractions that need to be applied to the edge of a sub-model will therefore be piecewise distributions, the number of pieces being equal to the number of full-model primitive elements that the sub-model boundary cuts. The traction modes on the edge of the sub-model, being continuous, are unable to model such a form of applied loading exactly and so the evidence of sub-modelling performance in the presence of basic traction modes, obtained using the element extraction approach, is utilised in the general sub\_model. The nature of the approximation of discarding higher-order modes of traction is investigated and the performance of the general sub-modelling technique evaluated.

Throughout the paper numerical examples are used to demonstrate and confirm the proposed methodologies and the paper closes in Section 4 with recommendations for further work.

## 2. APPLICATION OF CONSISTENT BOUNDARY CONDITIONS

The application of kinematic or static boundary conditions for hybrid-equilibrium elements is through the specification of edge displacement or traction modes. For the hybrid element considered here the internal stress fields are polynomial of finite degree  $p$ . The edges may be curvilinear, and edge displacements are also polynomial of degree  $p$ . The displacements are defined in terms of the complete set of Legendre polynomials,  $P_n$ , where  $n = 0, 1, \dots, p$  as in Eq. (1).

$$P_n(\mathbf{z}) = \sum_{i=0}^n \frac{(-1)^i (2n-2i)!}{2^n i!(n-i)!(n-2i)!} \mathbf{z}^{(n-2i)} \quad (1)$$

where  $N = n/2$  for  $n$  even and  $N = (n-1)/2$  for  $n$  odd [12], and  $\mathbf{z}$  is the non-dimensional edge parameter, ranging from  $-1$  to  $+1$ , based on a linear map. The first two polynomials (degree  $n=0$  and  $n=1$ ), for example, are  $P_0 = 1$  and  $P_1 = \mathbf{z}$ .

The Legendre polynomials, with values  $\pm 1$  at the ends of an edge, are used as the basis for normal and tangential edge displacements,  $\{u\}$ , so that displacements at a point  $\mathbf{z}$  on an edge are given as:

$$\{u\} = [V]\{v\} \quad (2)$$

where  $\{v\}$  is a vector of amplitudes for the displacement modes or *generalised displacements*.  $[V]$  is formed as the Kronecker product in Eq. (3) for the plate membrane element with curved edge displacements of degree  $p$ .

$$[V] = [P_0(\mathbf{z}) \quad P_1(\mathbf{z}) \quad P_2(\mathbf{z}) \quad \cdots \quad P_p(\mathbf{z})] \otimes \begin{bmatrix} c & s \\ -s & c \end{bmatrix} \quad (3)$$

where  $c$  and  $s$  are the direction cosines of the outward normal to the curved edge relative to a Cartesian frame of reference. The two rows of  $[V]$  refer, respectively, to the normal and tangential components of displacement.

Edge tractions are considered in polynomial form of degree  $p$ . Conjugate distributions of edge tractions  $\{t\}$  are defined in Eq. (4).

$$\{t\} = [G]\{g\} \quad (4)$$

where  $\{g\}$  is a vector of *generalised forces* and the columns of  $[G]$  form a dual basis to that for displacements. This means that edge work can be evaluated from the scalar product:

$$\{v\}^T \{g\} = \int_{edge} \{u\}^T \{t\} de = \{v\}^T \int_{edge} [V]^T [G] de \{g\} \Rightarrow \int_{edge} [V]^T [G] de = [I] \quad (5)$$

For a straight edge, the orthogonality of the Legendre polynomials in  $[V]$  implies that the dual basis is unique and that  $[G] = [V][S]$  where  $[S]$  is the diagonal scaling matrix defined in Eq. (6).

$$[S] = \left[ \int_{edge} [V]^T [V] de \right]^{-1} \quad (6)$$

The reciprocal of a diagonal coefficient,  $s_{rr}$ , of the scaling matrix is given in Eq. (7).

$$s_{rr}^{-1} = \int_{-\frac{l}{2}}^{\frac{l}{2}} P_i^2 de = \frac{l}{2} \int_{-1}^1 P_i^2 dz = \frac{l}{2} \cdot \frac{2}{(2i+1)} = \frac{l}{(2i+1)} \quad (7)$$

where  $r = (2i + 1)$ ,  $(2i + 2)$  and  $l$  is the edge length.

For a curved edge, however, the formation of  $[G]$  may be more problematic.

## 2.1 The General Case

The general case of application of boundary conditions occurs when they are determined from known displacement or stress fields. Thus, for example, KBCs might be derived from some applied displacement field,  $\{\tilde{u}\}$ , and SBCs from applied tractions  $\{\tilde{t}\}$  which might correspond to an applied stress field  $\{\tilde{S}\}$ .

### 2.1.1 Consistent KBCs.

Prescribed displacements  $\{\tilde{u}\}$  are mapped into consistent generalised displacements  $\{v\}$  by requiring that the same work be done by all generalised forces in moving by  $\{\tilde{u}\}$  or  $\{u\}$  ( $= [V]\{v\}$ ). This leads to Eq. (8).

$$\int_{edge} [G]^T \{\tilde{u}\} de = \int_{edge} [G]^T [V] de \cdot \{v\} = \{v\} \quad (8)$$

As a demonstration of the application of KBCs the isotropic non-polynomial displacement field of Eq. (9) is applied to the boundary of an isosceles triangle:

$$\{\tilde{u}\} = \frac{\sqrt{x^2 + y^2}}{2} \begin{Bmatrix} 1 \\ 1 \end{Bmatrix} \quad (9)$$

The displaced shapes are shown in Fig. 1 for increasing levels of  $p$ . With a non-polynomial displacement field the edge displacement modes cannot fit exactly but, instead, converge with decreasing vertex discontinuity as the edge displacement degree  $p$  is increased.

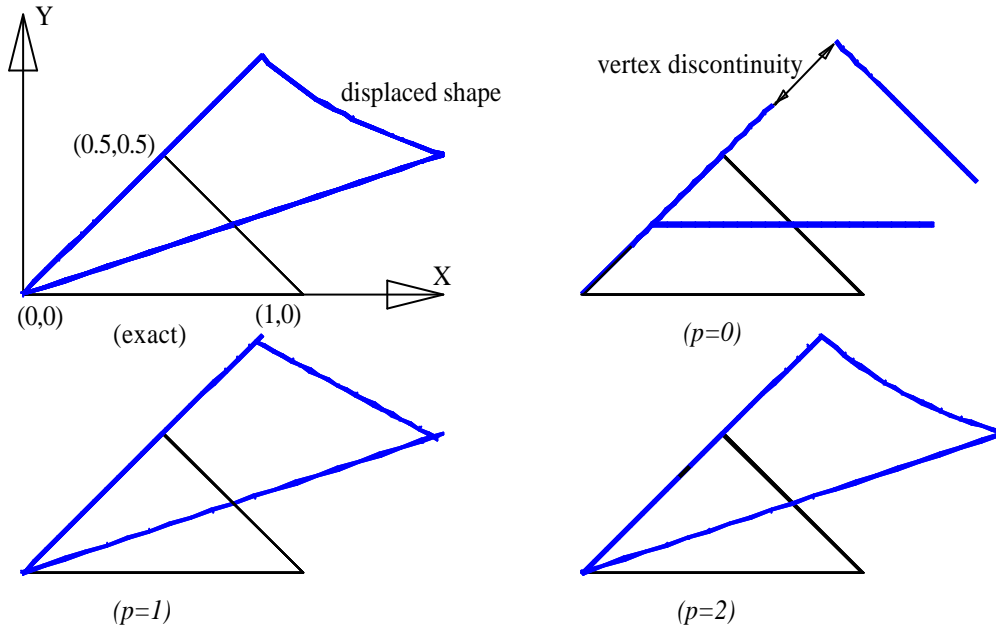


**Fig. 1.** Convergence of KBCs (general case).

### 2.1.2 Consistent SBCs

Prescribed tractions  $\{\tilde{t}\}$  are mapped into consistent generalised forces  $\{g\}$  by requiring that the same work be done by the prescribed tractions and  $\{t\}$  ( $= [G]\{g\}$ ) when displaced by all generalised displacements  $\{v\}$ . Thus:

$$\int_{edge} [V]^T \{\tilde{t}\} de = \int_{edge} [V]^T [G] de \{g\} = \{g\} \quad (10)$$

The generalised displacements should include the rigid body modes to ensure that the generalised forces are statically equivalent to the prescribed tractions. As a demonstration of the application of SBCs the non-polynomial (transcendental) stress field of Eq. (11) is used to define boundary tractions to the square region of Fig. 2.

$$\{\tilde{\mathbf{S}}\} = \begin{Bmatrix} \mathbf{s}_x \\ \mathbf{s}_y \\ \mathbf{t} \end{Bmatrix} = \frac{1}{2\sqrt{r}} \begin{Bmatrix} \cos \frac{\mathbf{q}}{2} (1 - \sin \frac{\mathbf{q}}{2} \sin \frac{3\mathbf{q}}{2}) \\ \cos \frac{\mathbf{q}}{2} (1 + \sin \frac{\mathbf{q}}{2} \sin \frac{3\mathbf{q}}{2}) \\ \sin \frac{\mathbf{q}}{2} \cos \frac{\mathbf{q}}{2} \cos \frac{3\mathbf{q}}{2} \end{Bmatrix} \quad (11)$$

where  $r$  and  $\mathbf{q}$  are polar ordinates.

This stress field is a Trefftz field (statically and kinematically admissible) and is for a plate with a crack centred at the origin (0,0). To avoid infinite stresses and therefore tractions, the region has been shifted 0.1 units in the positive X-direction.

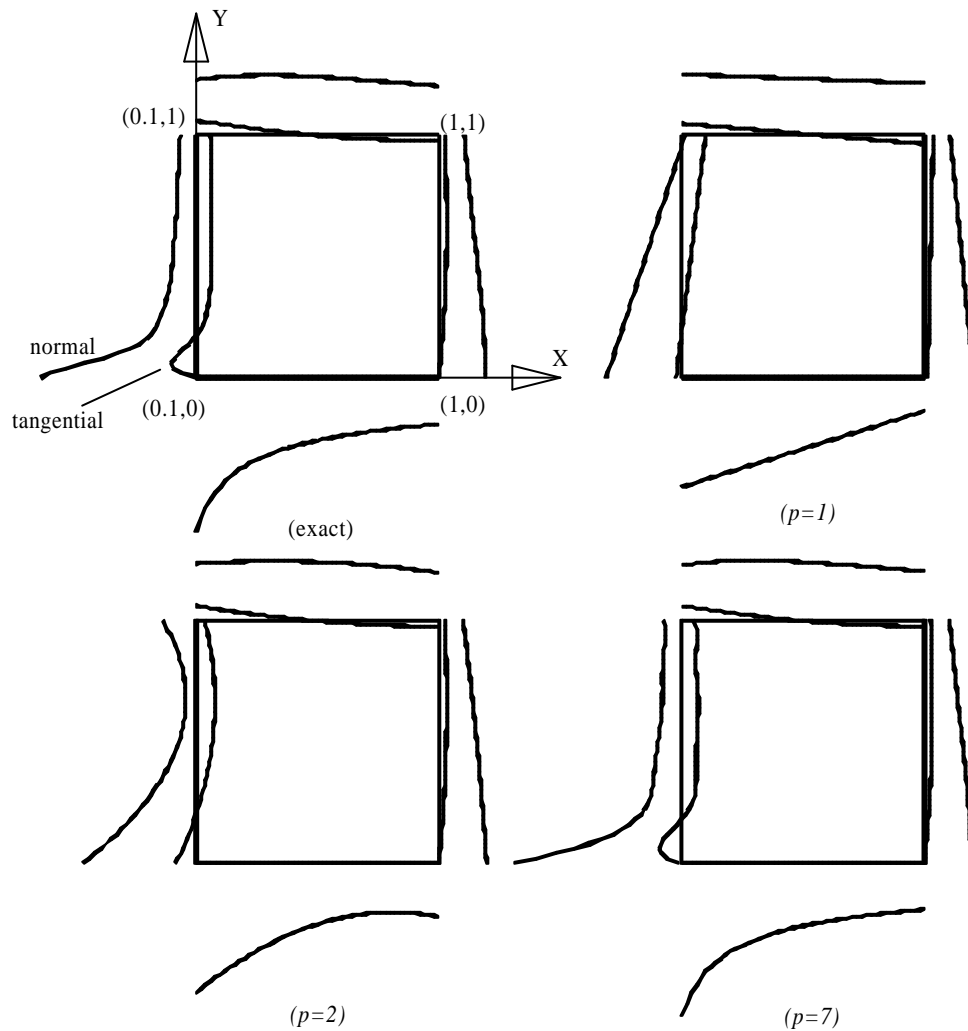


**Fig. 2.** Convergence of SBCs (general case).

The normal and tangential components of edge traction are plotted as distributions for each edge in Fig. 2. The convention used is indicated in Fig. 3 where a normal and tangential

vector pair is chosen such that the edge normal vector points away from the interior of the model with the tangential vector rotated  $90^\circ$  from the normal vector in the direction  $X$  to  $Y$ .

The normal and tangential tractions are distinguished in Fig. 2 by noting that the normal tractions have greater amplitude than the tangential ones.

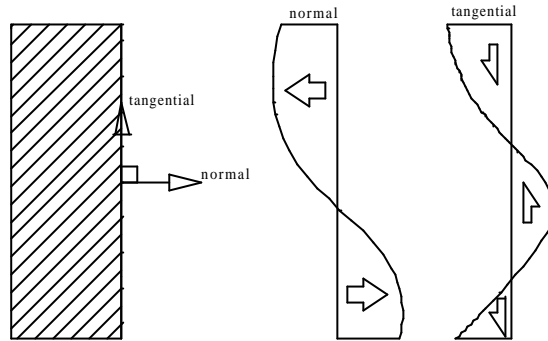


**Fig. 3.** Sign convention for edge tractions.

### 2.2 The Particular Case of Uniform $h$ -Refinement

Having established the consistent methodology for applying general forms of static and kinematic boundary conditions to an arbitrary mesh of equilibrium elements, the particular case of transforming these boundary conditions onto a uniformly refined mesh is now considered.

In uniform  $h$ -refinement an edge is divided into equal length portions as indicated in Fig. 4 for a straight edge divided into two.

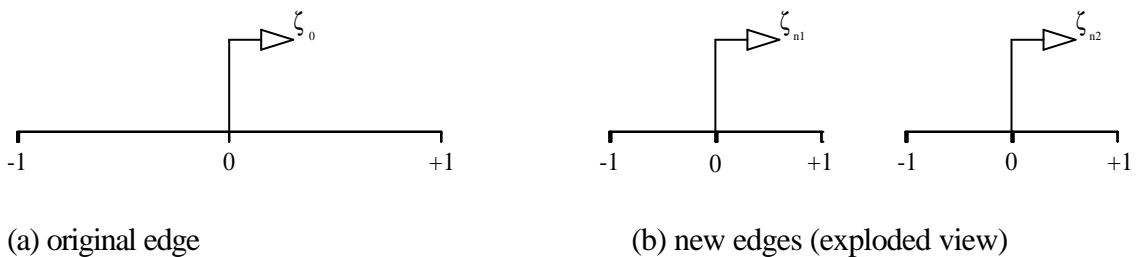


**Fig. 4.** Uniform  $h$ -refinement of an edge.

The non-dimensional ordinates are  $z_o$  for the original edge and  $z_{n1}$  and  $z_{n2}$ , respectively, for the two new edges.

When sub-modelling is considered in section 3, it will generally be necessary to distinguish between two types of edge, i.e. internal and external. In this context internal edges

become external for a sub-model whereas external edges remain external to the sub-model. The treatment of the boundary conditions on internal edges which become external must use the displacements or tractions derived from the results of the global model as boundary conditions.

External edges, on the other hand, will continue to use directly the prescribed boundary conditions. As a demonstration of the application of KBCs the triangle used earlier (see Fig. 1) is uniformly subdivided into three quadrilateral elements. Fig. 5 illustrates consistent KBCs for the refined models. It should be emphasised that each FE model cannot distinguish between the exact and the consistent KBCs. Fig. 5 illustrates how the displacement discontinuities converge towards zero with increasing  $p$ .

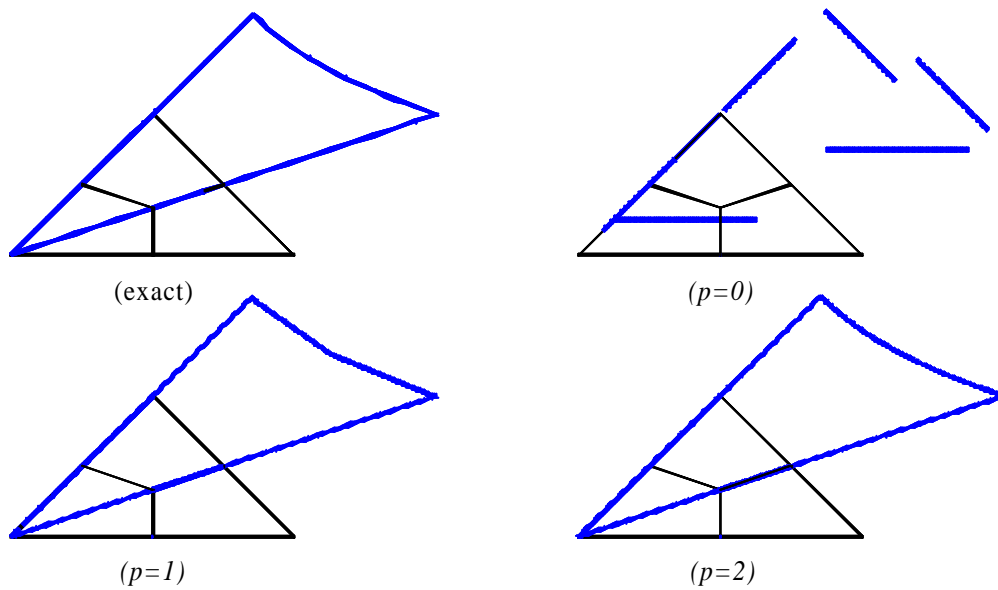


**Fig. 5.** Convergence of KBCs (particular case of uniform  $h$ -refinement).

Similarly, the square used earlier (see Fig. 2) is uniformly subdivided into four quadrilateral elements. Fig. 6 illustrates the consistent SBCs for the refined models. The traction discontinuities are observed to converge towards zero with increasing  $p$ .

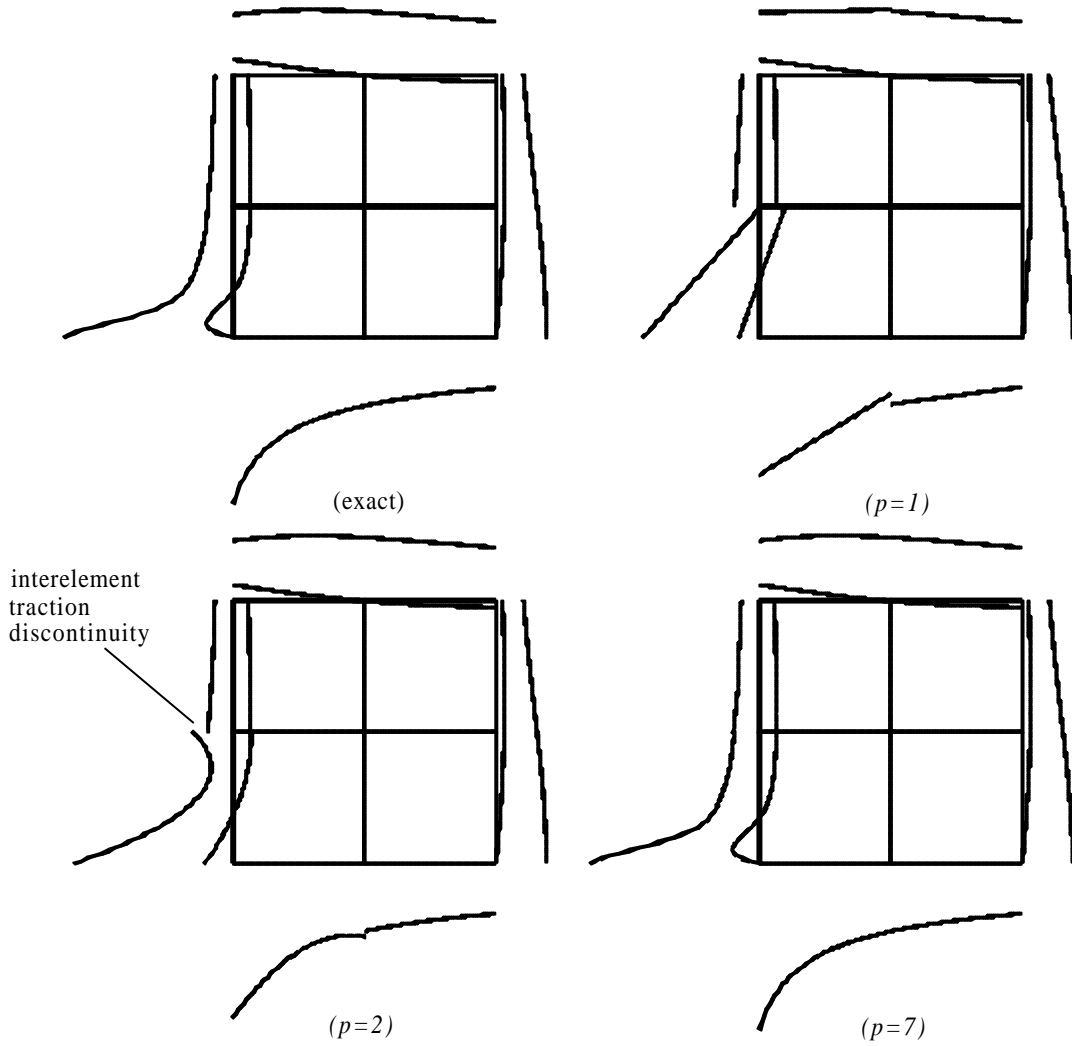


**Fig. 6.** Convergence of SBCs (particular case of uniform  $h$ -refinement).

### 2.2.1 KBCs for Internal Edges

For uniform  $h$ -refinement the boundary displacements on internal edges,  $\{\tilde{u}_n\}$ , are defined in terms of generalised displacements from the analysis of the global model:

$$\{\tilde{u}_n\} = [V_o] \{v_o\} \quad (12)$$

where the subscript  $o$  indicates an original edge.

The generalised displacements for a new edge,  $e_n$ , are:

$$\{v_n\} = [S_n]^T \int [V_n]^T \{\tilde{u}_n\} de_n = [S_n]^T \int [V_n]^T [V_o] de_n \{v_o\} \quad (13)$$

### 2.2.2 SBCs for Internal Edges

For uniform  $h$ -refinement the boundary tractions on internal edges,  $\{\tilde{t}_n\}$ , are defined in terms of generalised tractions from the analysis of the global model:

$$\{\tilde{t}_n\} = [V_o] [S_o] \{g_o\} \quad (14)$$

where the subscript  $o$  indicates the original edge.

The generalised forces for the new edge,  $e_n$ , are:

$$\{g_n\} = \int [V_n]^T \{\tilde{t}_n\} de_n = \int [V_n]^T [V_o] de_n [S_o] \{g_o\} \quad (15)$$

### 2.2.3 The Mapping Matrix

It is observed that the transformation of both kinematic and static boundary conditions from original to new edges (Eqs. 13 and 15) involve the same mapping matrix  $[M]$ , i.e.

$\{v_n\} = [S_n]^T [M] \{v_o\}$ , and  $\{g_n\} = [M] [S_o] \{g_o\}$  where:

$$[M] = \int [V_n]^T [V_o] de_n \quad (16)$$

After division of an edge into two equal lengths the transformations between original and new non-dimensional edge parameters are:

$$z_n = 2z_o \pm 1 \quad \text{or} \quad z_o = \frac{1}{2}(z_n \mp 1) \quad (17)$$

respectively for the new edges  $-1 \leq z_o \leq 0$  and  $0 \leq z_o \leq +1$ .

The coefficients  $M_{rs}$  are zero unless  $r, s = (2j - 1), (2i - 1)$  or  $2j, 2i$  for indices  $i, j$  which range from 0 to  $p$ . Then:

$$M_{rs} = \frac{l_n}{2} \int_{-1}^{+1} P_i(z_o) P_j(z_n) dz_n \quad (18)$$

where  $l_n$  is the length of the new edge. Such coefficients, when  $i$  and  $j$  range from 0 to 2, are given in Table 1.

**Table 1** : Integral terms in the mapping matrix

degree of Legendre polynomial		value of integral	
original	new	$\int P_i(z_o)P_j(z_n)dz_n$	
$i$	$j$	$-1 \leq z_o \leq 0$	$0 \leq z_o \leq +1$
0	0	2	2
0	1	0	0
0	2	0	0
1	0	-1	1
1	1	1/3	1/3
1	2	0	0
2	0	0	0
2	1	-1/2	1/2
2	2	1/10	1/10

### 2.3 Boundary Conditions in Practical Finite Element Analysis

The aforementioned methodology for applying boundary conditions derived from arbitrarily defined stress and displacement fields is ideally suited to the so-called *benchmarking* of a FE program. The provision of such routines within the code leads to a program with the capability of producing its own benchmark problems which, in addition to providing a ready source of problems with which to validate the code, offers a useful educational feature to the novice user.

In contrast to the inverse problem of deriving boundary conditions from known stress or displacement fields, practical FEA is generally concerned with finding the stress and/or displacements due to a particular form of applied loading. This loading is often rather simple in form involving, in terms of static variables little more than application of stress resultants, i.e. resultant forces and moments, and in terms of kinematic variables simple rigid-body restraints, or slightly more complicated forms to enforce conditions such as symmetry.

It is worth noting here a practical advantage of loading through element edge modes.

In conventional finite elements, where nodal variables are generally referenced to a global coordinate system, it is necessary, in order to apply conditions such as symmetry, to transform nodal variables into a local system which is normal and tangential to a model edge. In contrast to this, the edge displacement modes used for the equilibrium element are naturally aligned in this manner thereby simplifying the application of boundary conditions and avoiding potential user errors induced by incorrect specification of local freedoms.

In the majority of practical FEA the applied loading involves specification of nothing more than stress resultants. The reason for this is that the higher order modes of load are generally unknown and, through St Venant's principle, are usually not significant to the stress field remote from the region of loading.

If the stress resultants for an edge are  $N$ ,  $T$  and  $M$ , as illustrated in Fig. 7 for a straight edge, then the relationship between the stress resultants and the generalised forces is:

$$\begin{Bmatrix} N \\ T \\ M \end{Bmatrix} = \begin{bmatrix} 1 & 0 & 0 \\ 0 & 1 & 0 \\ 0 & 0 & l/2 \end{bmatrix} \begin{Bmatrix} g_1 \\ g_2 \\ g_3 \end{Bmatrix} \quad (19)$$

where  $l$  is the edge length and  $g_1$  to  $g_3$  are the first three components of  $\{g\}$  in Eq. (4).

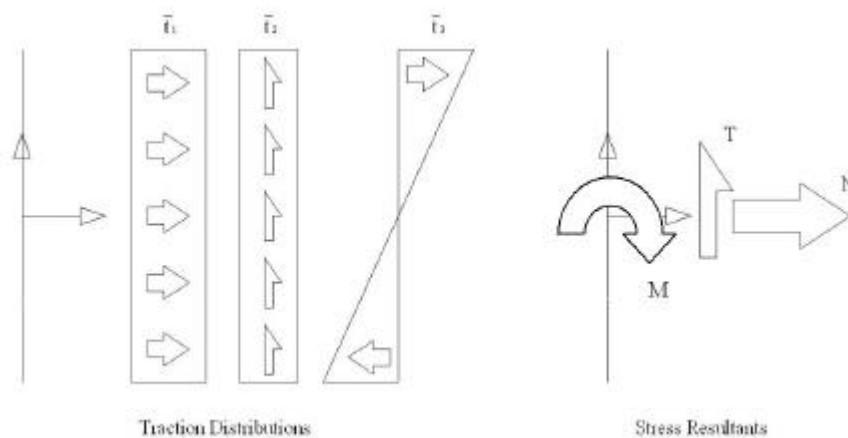


**Fig. 7.** Basic edge tractions modes and corresponding stress resultants for an edge.

### 3. SUB-MODELLING

The sub-modelling technique involves the generation of a refined sub-model which is then loaded with boundary conditions obtained from a full-model such that the solution quantity of interest, typically a point value of stress, may be obtained with superior accuracy. A straightforward approach to sub-model creation that is particularly suited to  $p$ -type elements is that of *element-extraction*. In this approach a relatively crudely discretised full-model is used with sufficient elements to capture the geometry of the problem and, perhaps, with some biasing towards regions of potential interest. The basic sub-model then constitutes a complete element of the full-model for which boundary conditions in the form of edge traction modes are readily available from the full-model results. The sub-model can then be refined with a mixture of  $p$ -refinement and  $h$ -refinement as appropriate. One could, of course, have performed such local refinement in the full-model, however, the element extraction technique offers a model of reduced computational size that is less likely to be affected by any potential ill-conditioning associated with local refinement of the full-model. A more general case of sub-model can be envisaged in which the sub-model boundaries do not lie along edges of the full-model. In this instance boundary conditions are not immediately available and some form of additional post-processing needs to be applied to the full-model results in order to achieve suitable sub-model loading.

#### *3.1 Sub-Modelling – A Classical Problem with Practical Significance*

A classical problem appropriate for the study of sub-modelling is that of the plate-membrane with a circular hole. The hole concentrates the stress and the aim is to obtain an accurate prediction of the peak stress. This problem characterises much of the routine FEA conducted in the field of practical mechanical engineering where, typically, such peak stresses limit the fatigue or creep life of a component. This problem has an analytical solution with

which the FE results may be compared if modelled correctly. Correct modelling requires that the boundary conditions be derived from the analytical stress field for the particular geometry of the FE model. The analytical stress field in Eq. (20) applies to an infinite plate subjected to a uniform uniaxial tension at infinity.

$$\begin{aligned}
 \mathbf{s}_x &= \mathbf{s}_\infty \left\{ 1 - \frac{a^2}{r^2} \left( \frac{3}{2} \cos 2\mathbf{q} + \cos 4\mathbf{q} \right) + \frac{3}{2} \frac{a^4}{r^4} \cos 4\mathbf{q} \right\} \\
 \mathbf{s}_y &= \mathbf{s}_\infty \left\{ 0 - \frac{a^2}{r^2} \left( \frac{1}{2} \cos 2\mathbf{q} - \cos 4\mathbf{q} \right) - \frac{3}{2} \frac{a^4}{r^4} \cos 4\mathbf{q} \right\} \\
 \mathbf{t}_{xy} &= \mathbf{s}_\infty \left\{ 0 - \frac{a^2}{r^2} \left( \frac{1}{2} \sin 2\mathbf{q} + \sin 4\mathbf{q} \right) + \frac{3}{2} \frac{a^4}{r^4} \sin 4\mathbf{q} \right\}
 \end{aligned} \tag{20}$$

where  $r$  and  $\mathbf{q}$  are polar position ordinates,  $a$  is the hole radius and  $\mathbf{s}_\infty$  is the (uniform) value of  $\mathbf{s}_x$  at  $r = \infty$ .

For a plate of finite dimensions, the distribution of stress on the boundaries is non-uniform and whilst the problem is often modelled by assuming uniform traction distributions, the analytical solution is only valid when the non-uniform distributions are taken into account. The non-uniformity of the traction distributions, which is only of practical significance when the dimension of the hole approaches that of the plate, are evident for the problem investigated here where the dimension are chosen such that the plate is square of semi-length,  $l$ , and the ratio of semi-length to hole radius is 5.

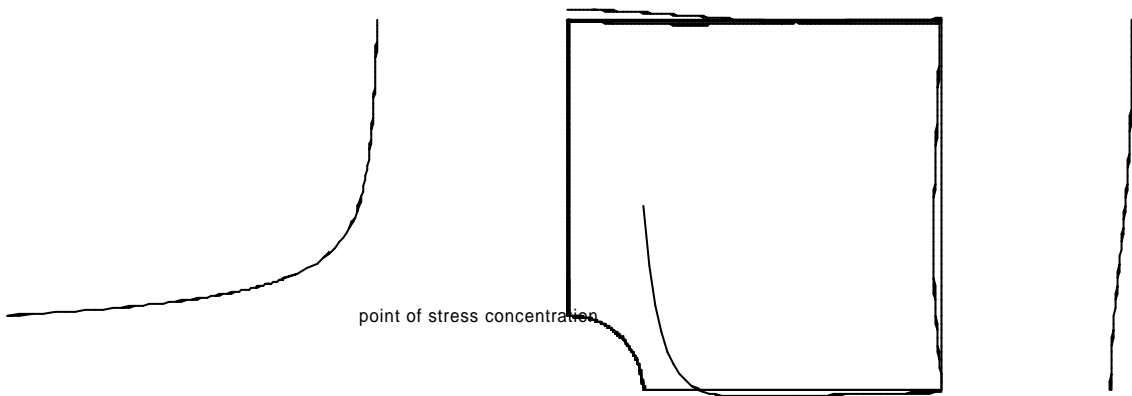


**Fig. 8.** Analytical boundary tractions around the quarter plate.

The FE model used for this problem utilises symmetry by modelling only a quarter of the plate. The boundary tractions due to the analytical stress field are shown for the quarter plate in Fig. 8 where the normal tractions are distinguished by their dominance over the tangential traction components. Although SBCs are known around the entire boundary, edges lying on the planes of symmetry will be constrained with symmetric KBCs in all analyses.

The quarter plate is designated as the full-model and the FE meshes are shown in Fig. 9. The basic mesh, designated as  $h=0$ , consists of six elements with a biasing towards the point of stress concentration. The other two meshes are successive uniform refinements of this basic mesh. The element extracted for the sub-model is shown shaded in the basic mesh.

Another form of approximation concerns modelling the shape of the circular hole. Most types of finite element, including the equilibrium element considered here, use polynomial forms for element edges. For this example a quadratic form of edge will be used. The analytical solution in Eq. (20) remains valid for the FE model provided corresponding non-zero tractions are derived and applied to the perimeter of the hole as modelled.

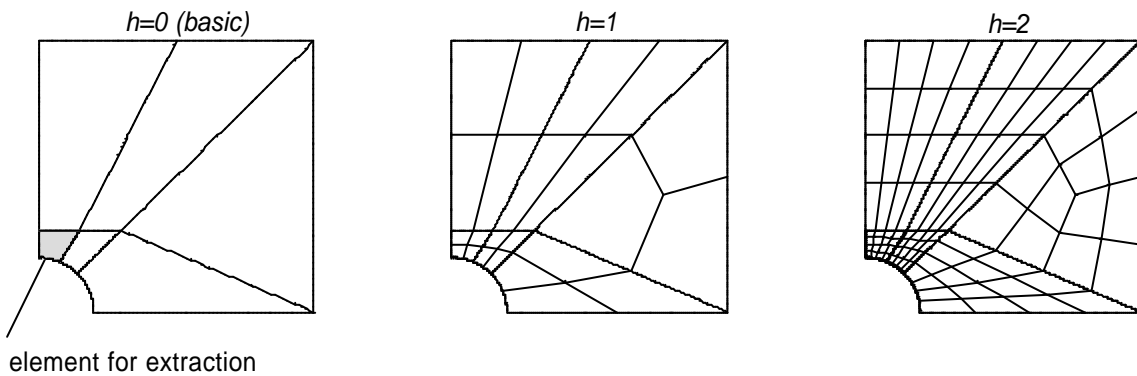


**Fig. 9.** Finite element meshes – full-model.

The tractions applied to all the FE approximations of the circular arc are shown for the basic mesh in Fig. 10. In this case the arc is approximated by three piecewise quadratic edges defined so that end and centre points lie on the arc. The tangential tractions are more

significant than the normal ones and the discontinuity in slope between adjacent edges leads to the discontinuities in traction seen in the figure.

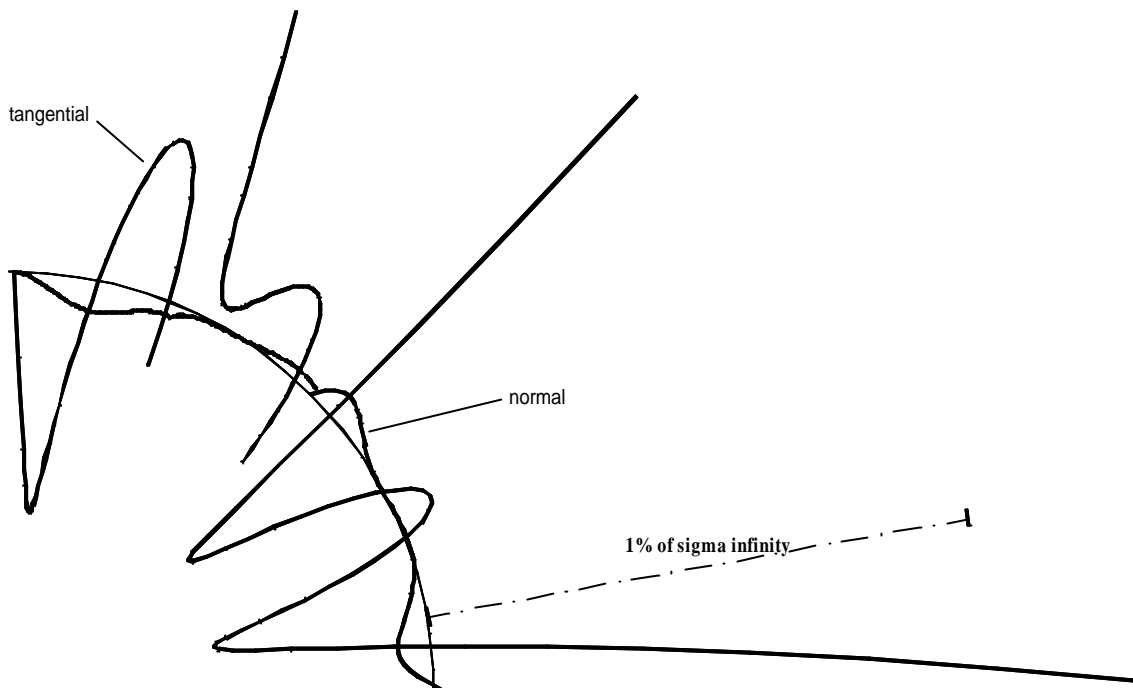


**Fig. 10.** Analytical boundary tractions around the FE approximations of the circular arc.

In this particular problem the quantity of interest is the value of  $\mathbf{s}_x$  at the top of the arc where it has an exact value of  $3\mathbf{s}_\infty$ . The performance of the full-model under  $p$ - and  $h$ -refinement is shown in Fig. 11 where contour plots of  $\mathbf{s}_x$  are shown together with the maximum value of this quantity when  $\mathbf{s}_y = 1$ . Rapid convergence of the quantity of interest is observed with both forms of refinement. The stress fields within elements exhibit internal discontinuities particularly for lower levels of refinement. These occur because the elements used are actually macro elements consisting of an assemblage of triangular primitives as discussed in section 3.3.

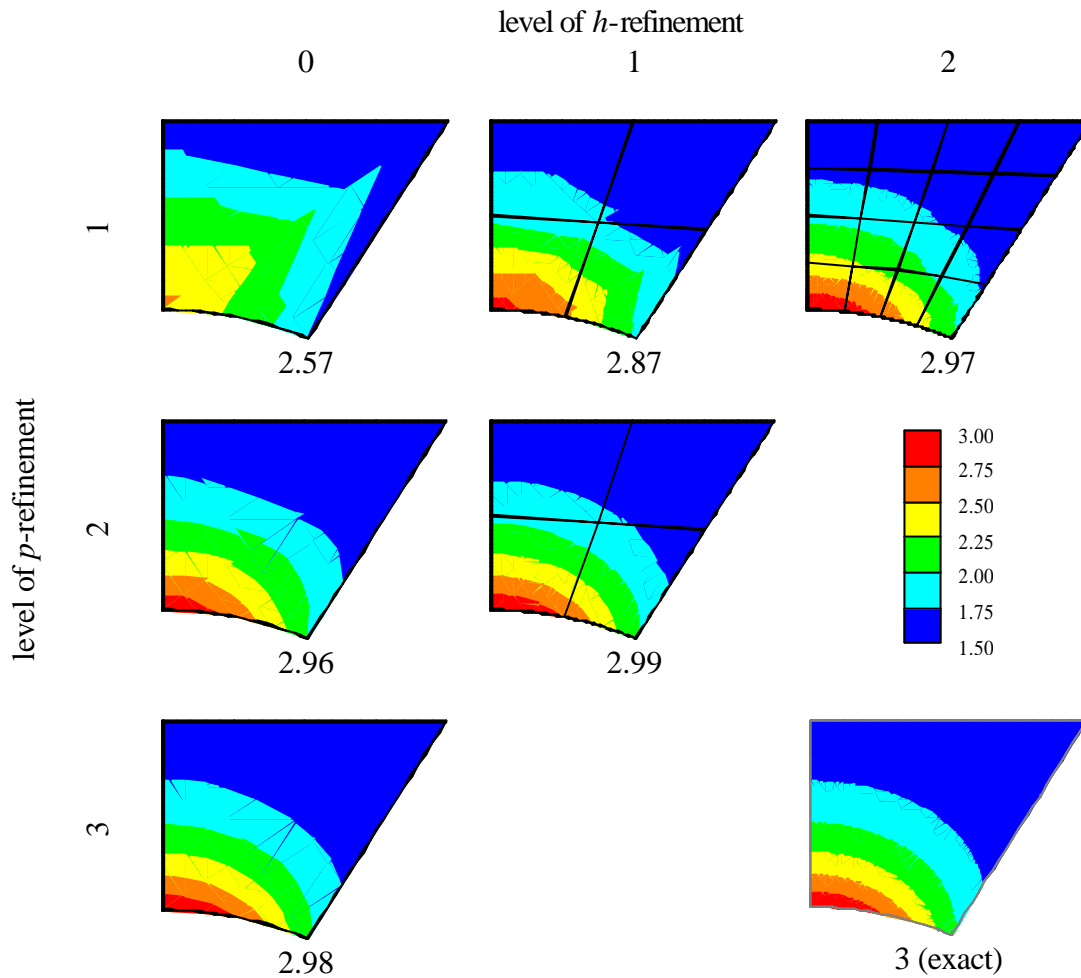


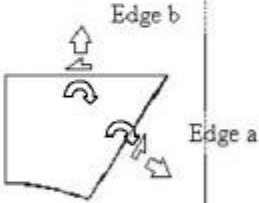
**Fig. 11.** Convergence of  $s_x$  for full-model.

### 3.2 Sub-Modelling – Particular Case of Element Extraction

This form of sub-modelling involves a sub-model constituting the region of a complete element in the full-model with SBCs taken directly in the form of edge traction modes from the full-model when  $p = 1$ . The performance of the sub-model, identified in Fig. 9, under  $p$ - and  $h$ -refinement is shown in the left-hand portion of Fig. 13.

The first sub-model mesh ( $p=1$ ,  $h=0$ ) produces, as expected, identical results to the corresponding full-model. The convergence of the quantity of interest with both types of refinement is strong but appears to be towards a value of 2.85 rather than the exact value of 3.00. This is not unexpected as the full-model, which was used to provide the boundary conditions for all these sub-models, was fairly crude and the amplitudes of the basic tractions

were different from what they should have been – see Fig. 12. It is pleasing, however, to note that the improvement in the result is significant (just short of 10% of the exact value) and is in the correct direction. Convergence of sub-models to the exact value using full-models of higher degrees of  $p$ -refinement, although not reported here, has been confirmed.

		level of $h$ -refinement						
		0		1		2		
		a	b	a	b	a	b	
level of $p$ -refinement	1	$N$	1.9270	0.3971	1.9013	0.3890		
		$T$	0.7585	-0.0533	0.7514	-0.0534		
		$M$	-0.1438	0.0393	-0.1854	0.0539		
	2	$N$	1.9150	0.4015	1.8917	0.3802		
		$T$	0.7454	-0.0519	0.7556	-0.0397		
		$M$	-0.1852	0.0528	-0.1867	0.0600		
	3	$N$	1.8980	0.3873			1.8908	0.3781
		$T$	0.7516	-0.0429			0.7578	-0.0350
		$M$	-0.1862	0.0580			-0.1867	0.0622
						(exact)		

**Fig. 12.** Convergence of internal edge stress resultants for full model.

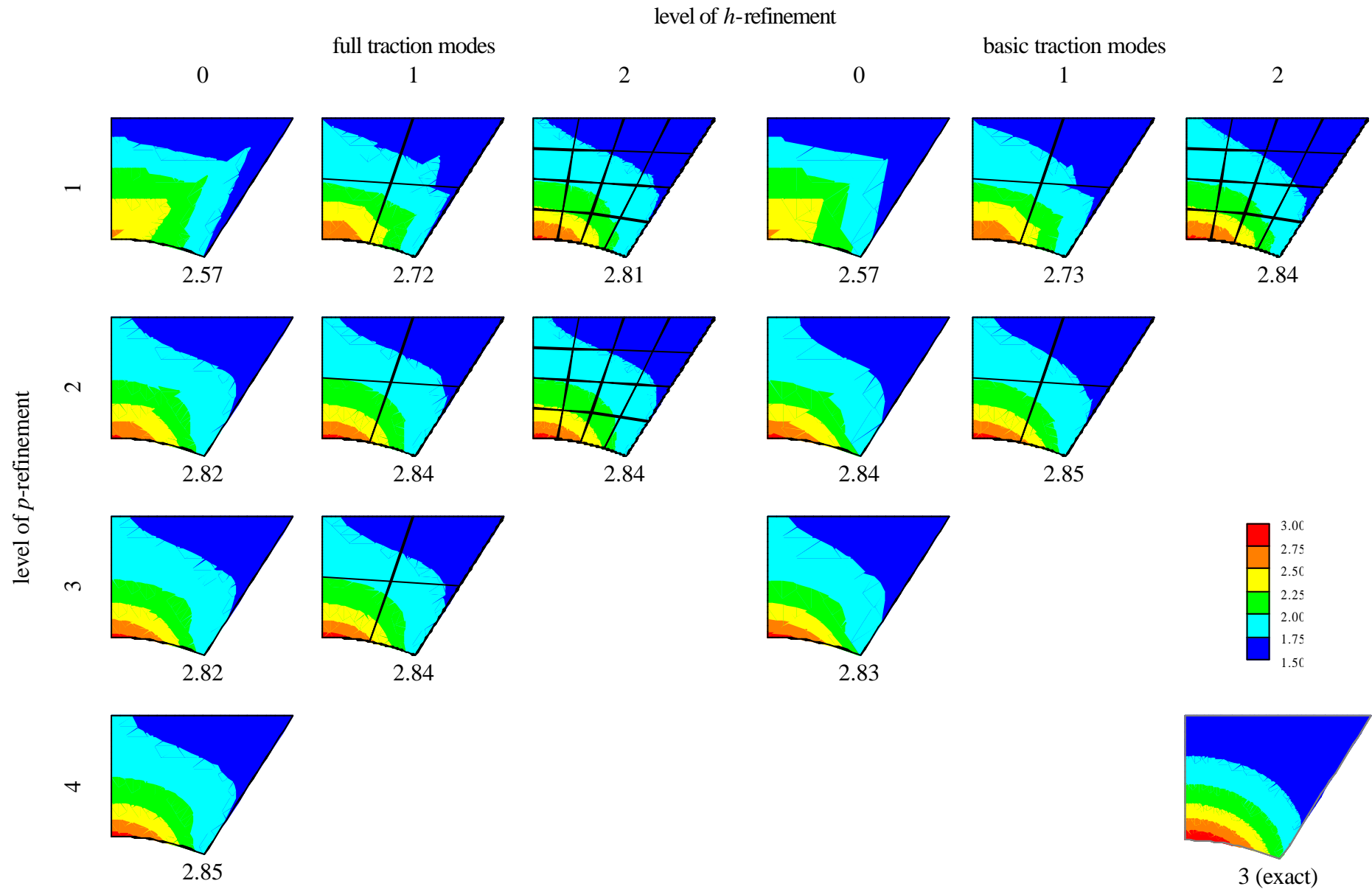


**Fig. 13.** Convergence of  $s_x$  for sub-model - full tractions from full-model with  $p=1$ ,  $h=0$ .

### 3.2.1 Sub-Modelling – Element Extraction with Basic Traction Modes

As already noted, the only traction modes required to transfer overall equilibrium between elements are the basic tractions. The so-called *higher-order* traction modes are self-balancing on an element edge and only influence the stress field local to the edge.

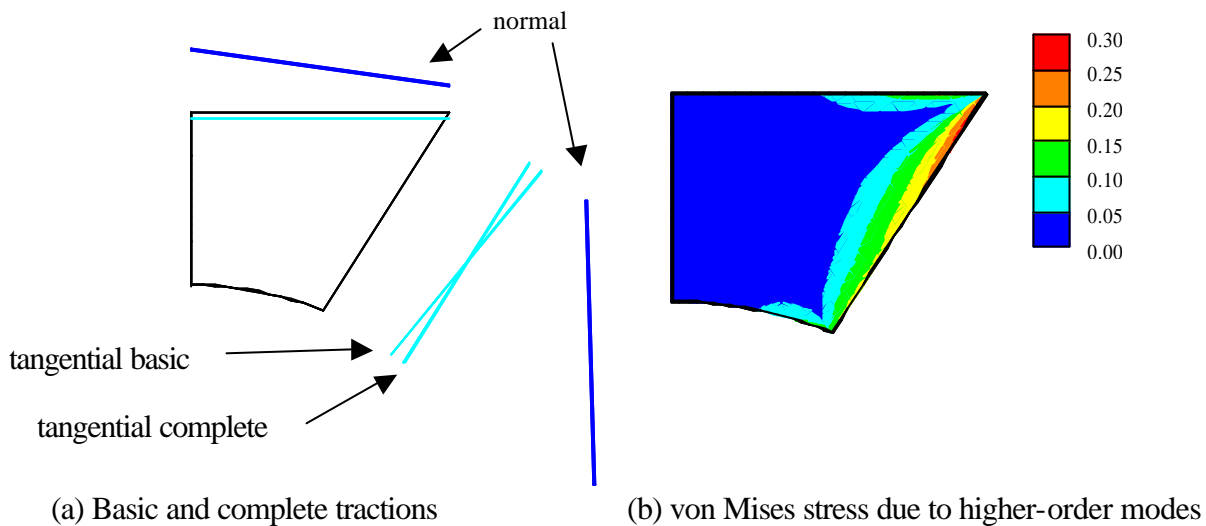


**Fig. 14.** Basic and complete tractions for sub-model - full-model with  $p=1$ ,  $h=0$ .

The performance of the sub-model under  $p$ - and  $h$ -refinement and using basic tractions only is shown in the right-hand portion of Fig. 13. The results are interesting in that although loaded with the higher-order tractions removed, the results for the quantity of interest are no worse and in most cases a little better than those produced using the complete set of tractions. The difference between complete and basic tractions is illustrated in Fig. 14(a) for  $p=1$ . The linear tangential traction modes (these being the only higher-order modes present for a linear element) are set to zero on edges  $a$  and  $b$ . In this particular example these quantities are small and a measure of the effect of the higher-order modes on the stress field is given in Fig. 14(b) which shows the von Mises stress contours resulting from the higher-order traction modes acting alone.

### 3.3 Sub-Modelling – General Case

In the general case of sub-modelling the edges of the sub-model may cut across the boundaries of elements in the full-model. Such edges form a *model section* which may be arbitrary. As the stress field is generally not continuous across interelement boundaries a method for applying boundary tractions to the sub model will need to cope with discontinuous boundary tractions. The issue of discontinuous stress fields is exacerbated by the fact that equilibrium elements are actually macro elements formed, respectively for the triangle and quadrilateral macros, from three and four triangular primitive elements as shown in Fig. 15. The primitive element boundaries form lines of potential stress discontinuity as observed in the contour plots of Fig. 11 and Fig. 13 in particular for the less refined models.

The position of the macro assembly point,  $P$ , can be chosen arbitrarily for the triangular macro but, in order to avoid malignant spurious kinematic modes (see reference [4]), for the piecewise linear quadrilateral, must be located at the intersection of the diagonals as indicated by dotted lines in the figure. For all problems considered in this paper, where the quadrilateral is used and for all degrees of internal stress field considered, the intersection of the diagonals locates  $P$ .

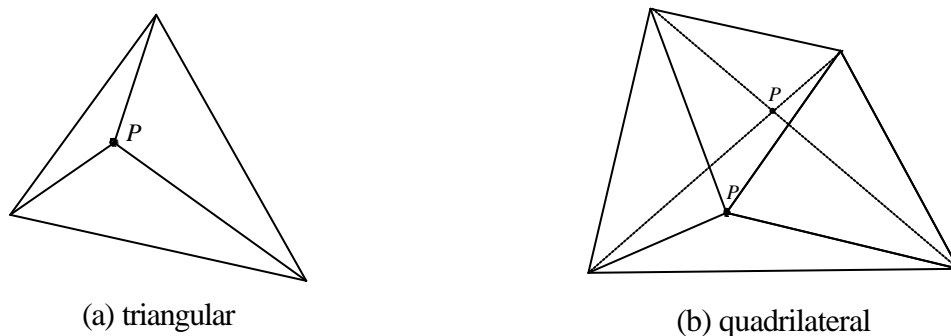


**Fig. 15.** Standard geometric forms of macro element.

#### 3.3.1 Sub-Modelling – Basic Traction on a Model Section

As already described, the FE stresses along an arbitrary model section through part or all of the model will, generally, be discontinuous. If a model section represents an edge of a sub-model

then the method of mapping to consistent continuous statically equivalent tractions needs to be adopted. As already demonstrated, higher-order traction modes are not strictly required for satisfactory sub-model performance and it is then sufficient for current purposes to establish only basic tractions along an arbitrary model section. This is achieved, for a straight edge, by use of Eq. (10) with the columns of  $[V]$  corresponding to displacements representing the three rigid-body modes.

An example applying this method is shown in Fig. 16. The full-model of the (quarter) plate with circular hole is used and the model section is defined to lie from (1,9) to (9,1). As in the plotting of edge stresses presented previously, the stresses are plotted normal to the section according to a section coordinate system defined as for an edge. The piecewise distributions of normal and tangential stress are shown together with the *linearised* distributions which correspond to the stress resultants that are statically admissible with the piecewise distributions.

With the section coordinate system used, and for the particular distributions of stress, the normal stresses lie below the section whilst the tangential stresses lie above it. The magnitudes of the section stress resultants (see Eq. (19)) are also listed in Fig. 16. The piecewise traction discontinuities are observed to decrease with increasing  $p$ .

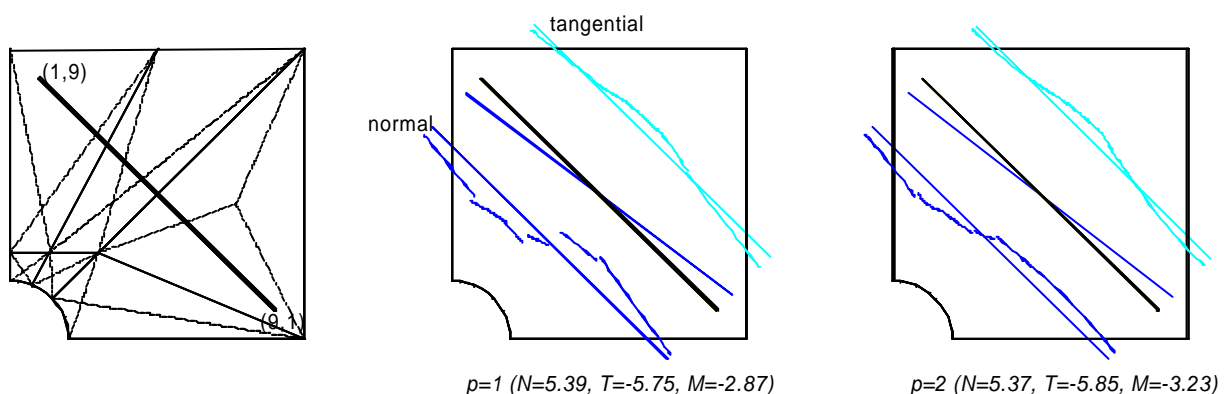


**Fig. 16.** Actual and basic tractions on a model section.

The method of stress linearisation is common in the context of structural design assessment where it is used to obtain membrane and bending stresses the magnitudes of which can be compared with allowable material values. The method finds particular application in pressure vessel design and analysis involving axisymmetric models. It is worth noting in this context that with the strong form of equilibrium offered by equilibrium elements, sections that arbitrarily bisect the structure will always provide stress resultants in equilibrium with the applied loading irrespective of the level of mesh refinement. Contrast this with the displacement element where although nodal forces provide an equilibrium set, element stresses integrated in the manner described above over an arbitrary bisecting section will not generally equilibrate with the applied loading until the mesh is sufficiently refined. The practice of generating membrane and bending sectional forces in this way is wide-spread in FEA based on displacement elements, and can lead to disastrously erroneous results as occurred with the design of the Sleipner platform [13]. The reason that the stress resultants shown along the section in Fig. 16 change with mesh refinement is that the section does not bisect the structure.

The more general case for sub-modelling is demonstrated by varying the sections which define edges a and b of the single element sub-model in section 3.2. Vertex  $v$  joining these two edges, as indicated in Fig. 17, is moved in a direction at  $45^\circ$  to the  $X$ -axis. Small perturbations  $\Delta_x$  and  $\Delta_y$  in the coordinates of  $v$  are considered in order to assess the sensitivity of the quantity of interest to such perturbations. The results for  $\Delta_x = \Delta_y = \pm 0.2$  are compared with that of the unperturbed geometry ( $\Delta_x = \Delta_y = 0$ ) in Fig. 17. The results for the unperturbed geometry are the same as presented in the right-hand side of Fig. 13 ( $p=1, h=0$ ). The results for the perturbed geometry produce peak values of  $\mathbf{s}_x$  that are virtually identical to those from the unperturbed geometry.

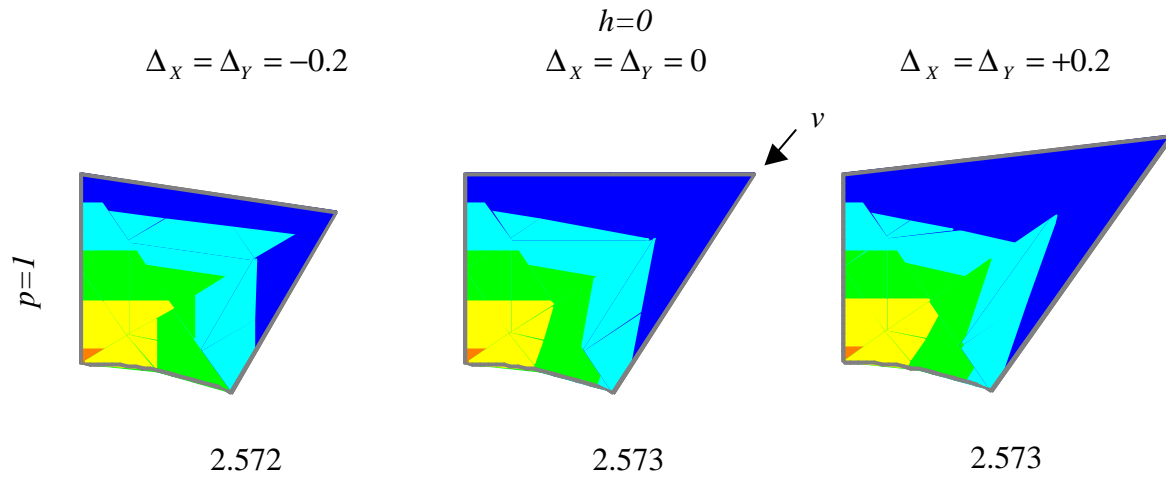


**Fig. 17.** Variation of  $S_x$  for sub-model - full-model with  $p=1$ ,  $h=0$ .

#### 4.0 Conclusions

The motivation for conducting the work presented in this paper was to establish and demonstrate a methodology for sub-modelling using equilibrium elements. In order to do this it was necessary to consider how boundary conditions, both kinematic and static, are applied to such elements and how they are inherited from a parent mesh to its uniformly refined child mesh. A simple form of sub-modelling using an element-extraction approach was then demonstrated both in the presence of complete and partial or basic traction modes. Both sets of tractions provided similar results demonstrating the feasibility of using basic tractions alone for general sub-modelling where sub-model edges do not coincide with edges in the parent model. In preparing a methodology for sub-modelling in the general case a scheme for extracting stress resultants from an arbitrary model section was required. This scheme was then used to determine the amplitudes of the basic traction modes for sub-models having slightly perturbed geometry from that used previously. In this manner the general method of sub-modelling was demonstrated.

The results presented in this paper indicate that it is possible to obtain good quality point quantities by using a relatively coarse and low degree full-model followed by sub-model analysis in the region of interest. The results suggest that it is not necessary to use complete sets of traction

modes on the sub-model boundary and that the basic ones are sufficient. It also appears that for the sub-model, high levels of refinement are unnecessary. The expected superiority of  $p$ - over  $h$ -refinement is observed with two levels of  $h$ -refinement being required to achieve the improvement in solution gained by only one level of  $p$ -refinement. A recommended refinement strategy in the sub-modelling technique might then assume that converged results will be achieved by unit increase in both  $h$  and  $p$ .

Further development of equilibrium elements continues to suggest distinct advantages over the corresponding displacement type element. For example, a mesh invariant ability to provide statically admissible stress resultants on an arbitrary model section leads to a safe method of structural assessment in linear-elastic FE analysis which has been known to fail with the more conventional displacement elements. It is of value, therefore, to explore these ideas further and this, together with the consideration of sub-modelling with other types of equilibrium element, will form the basis for future work.

### **Acknowledgement**

The authors would like to express their thanks to the reviewers of this paper for a number of thoughtful comments and suggestions which have significantly enhanced this paper.

## REFERENCES

- [1] ASME Pressure Vessel Code
- [2] M. Ainsworth, J.T. Oden, A Posteriori Error Estimation in Finite Element Analysis, Wiley, 2000.
- [3] J. Robinson, The mode-amplitude technique and hierarchical stress elements – a simplified and natural approach. *International Journal for Numerical Methods in Engineering*, 21: 487-507, 1985.
- [4] E.A.W. Maunder, J.P.B. Moitinho de Almeida and A.C.A. Ramsay, A General Formulation of Equilibrium Macro-Elements with Control of Spurious Kinematic Modes: the exorcism of an old curse, *International Journal for Numerical Methods in Engineering*, 39, 3175-3194, 1996.
- [5] E.A.W. Maunder and A.C.A. Ramsay, A Basis for an Axisymmetric Hybrid-Stress Element, *Strojnický Casopis*, 54, 263-276, 2003.
- [6] E.A.W. Maunder, Hybrid elements in the modelling of plates, in B.H.V. Topping, ed., *Finite Elements: Techniques and Developments*, Civil-Comp Press, 165-172, 2000.
- [7] J.P. Moitinho de Almeida, O.J.B. Almeida Pereira, A set of hybrid equilibrium finite element models for the analysis of three-dimensional solids. *International Journal for Numerical Methods in Engineering*, 39: 2789-2802, 1996.
- [8] J. Robinson, The CRE method of element testing and the Jacobian shape parameters, *Engineering Computations*, 4, 113-118, 1987.
- [9] J. Robinson, E.A.W. Maunder, Introduction to the S-adaptivity method, *Finite Elements in Analysis and Design*, 27, 163-173, 1997.
- [10] R.D. Cook, D.S. Malkus, M.E. Plesha, R.J. Witt, *Concepts and Applications of Finite Element Analysis*, Wiley, 4<sup>th</sup> edition, 2002.
- [11] A.C.A. Ramsay, E.A.W. Maunder, Boundary conditions and sub-modelling with p-type hybrid equilibrium plate elements. In the *International Conference on Adaptive Modeling and Simulation, ADMOS 2005*, P. Diez & N.-E. Wiberg, eds. CIMNE, 2005.
- [12] L.A. Pipes, *Applied Mathematics for Engineers and Physicists*, McGraw-Hill, 1958.
- [13] T. Kvamsdal, K.M. Mathisen, K.M. Okstad, H.B. Aas, Techniques for reliable calculation of sectional forces. In *FEM today and the future*, edited by J. Robinson, 450-456. Bridestowe: Robinson & Associates, 1993.